

TURBULENT HEAT TRANSFER IN THE THERMAL ENTRANCE REGION OF CONCENTRIC ANNULI WITH UNIFORM WALL HEAT FLUX

ALAN QUARMBY and R. K. ANAND

University of Manchester Institute of Science and Technology

(Received 9 October 1968)

Abstract—The problem of turbulent heat transfer in concentric annuli is analysed for the case in which there is a uniform heat flux at either annular surface. The solution is given for the thermal entrance region and the fully developed situation and may be extended by the principle of superposition to cases in which there are arbitrary axial variations in the wall heat flux at both annular surfaces.

The solutions are given for radius ratios 2.88, 5.625, 9.37 and 50 with Reynolds numbers from 20000 to 240000 and for $Pr = 0.01, 0.7$ and 1000. There is good agreement with experimental results for annuli for $Pr = 0.7$ whilst some results for a radius ratio equal to 50 compare favourably with results for a circular tube for other Prandtl numbers.

NOMENCLATURE

<p>A, cross sectional area of annulus;</p> <p>a, ratio of r_m/r_i;</p> <p>b, radius ratio r_o/r_i;</p> <p>C_p, specific heat at constant pressure;</p> <p>D, annulus characteristic dimension $2(r_o - r_i)$;</p> <p>$G(R)$, temperature solution for heating at the inner wall;</p> <p>$H(R)$, temperature solution for heating at the outer wall;</p> <p>h, heat-transfer coefficient;</p> <p>K, Von Kármán's constant in similarity hypothesis;</p> <p>k, thermal conductivity;</p> <p>l, mixing length in Jenkins expression;</p> <p>n, index in sublayer profile;</p> <p>Nu, Nusselt number hD/k;</p> <p>Pr, Prandtl number $\mu C_p/k$;</p> <p>q, wall heat flux;</p> <p>Re, Reynolds number $u_b D/v$;</p> <p>R, non dimensional radius $r/(r_o - r_i)$;</p> <p>r, radius;</p> <p>r_o^+, $r_o \sqrt{(\tau_o/\rho)/v}$;</p> <p>$t$, temperature;</p>	<p>T, non dimensional temperature $(t - t_e)/(qD/k)$;</p> <p>u, fluid velocity;</p> <p>u^+, non dimensional fluid velocity $u/(\tau/\rho)$;</p> <p>u_b, bulk velocity $1/A \int u dA$;</p> <p>v', fictitious velocity of spherical turbulent eddy;</p> <p>x, axial distance;</p> <p>x^+, non dimensional axial distance x/D;</p> <p>y, radial distance from annulus wall;</p> <p>y, $y \sqrt{(\tau/\rho)/v}$.</p> <p>Greek</p> <p>α, thermal diffusivity;</p> <p>β, $1 - y^+/y_m^+$;</p> <p>ρ, density;</p> <p>τ, shear stress;</p> <p>μ, viscosity;</p> <p>ν, kinematic viscosity;</p> <p>ϵ_m, eddy diffusivity of momentum;</p> <p>ϵ_H, eddy diffusivity of heat.</p> <p>Subscripts</p> <p>i, inner;</p> <p>o, outer;</p>
--	---

- m , at position of maximum velocity;
 ρ , at edge of sublayer;
 e , entrance value at $x = 0$;
 b , bulk value.

THE IMPORTANCE of the thermal entrance region in turbulent heat transfer in ducts is well established and solutions to the problem have been given for the circular tube and parallel plate channel for various thermal boundary conditions. The annular configuration is of great practical importance. Leung *et al.* [1] have presented a solution for the fully developed case with uniform heat flux at the annular walls but a complete solution for the thermal entrance region with this boundary condition has not been given previously.

In analysing such problems by use of the energy equation, it is necessary to have an accurate description of the turbulent velocity profile and eddy diffusivity variation in the duct. In the annulus there has been much experimental work carried out but conclusions about the velocity profile and eddy diffusivity have been rather conflicting. This is discussed by Quarmby [2]. The experimental results of [2] attempted to answer some of the questions raised by previous work. For example, it was shown that the turbulent velocity profile in annuli has both a radius ratio and a Reynolds number dependence. The radius of maximum velocity is not the same in turbulent flow as in laminar flow, nor may it be given in terms of the radius ratio only.

An analysis of turbulent flow in concentric annuli, based on Von Kármán's similarity hypothesis, has been given by Quarmby [3], which is in good agreement with the experimental findings of [2]. This analysis is used in the present work to provide a solution for the thermal entrance region heat transfer problem in a concentric annulus for the boundary condition that there is a uniform heat flux at either annular surface. The asymptotic solution for large values of the axial distance along

the duct gives results for the fully developed situation. Further, the principle of superposition allows the basic solution to be extended to give the solutions for cases in which there is any arbitrary axial variation of heat flux at the walls. Such cases of axial variation are of considerable practical interest.

GENERAL ENERGY EQUATION

The energy equation may be written

$$\frac{1}{r} \frac{\partial}{\partial r} \left[(\alpha + \varepsilon_H) r \frac{\partial t}{\partial r} \right] = u \frac{\partial t}{\partial x} \quad (1)$$

if the assumptions are made of constant fluid properties and negligible axial conduction. It is further assumed that the turbulent velocity profile is fully developed at the entrance to the heated section and that the entering fluid temperature is uniform, t_e . Equation (1) is made non-dimensional by use of

$$R = \frac{r}{r_o - r_i}, \quad x^+ = \frac{x}{D}, \quad r_o^+ = \frac{r_o \sqrt{(\tau_o)/\rho}}{v}$$

and

$$u_o^+ = u \sqrt{\left(\frac{\tau_o}{\rho}\right)}, \quad T = (t - t_e) \frac{qD}{k}$$

so that

$$\frac{1}{R} \frac{\partial}{\partial R} \left[\left(\frac{\varepsilon_H}{v} + \frac{1}{Pr} \right) R \frac{\partial T}{\partial R} \right] = \frac{b-1}{2b} r_o^+ u_o^+ \frac{\partial T}{\partial x^+} \quad (2)$$

For heating on the inner wall the temperature solution is denoted $T_i = (t - t_e)/(q_i D/k)$ and for the outer wall heated, correspondingly, $T_o = (t - t_e)\sqrt{(q_o D/k)}$.

The solution of equation (2) may be expressed as the sum of a fully developed part, T_1 , and a developing part, T_2 .

For heating on the inner wall T_i is given by

$$\frac{1}{R} \frac{\partial}{\partial R} \left[\left(\frac{\varepsilon_H}{v} + \frac{1}{Pr} \right) R \frac{\partial T_i}{\partial R} \right] = \frac{2(b-1) r_o^+ u_o^+}{b(b+1) Re Pr} \quad (3)$$

where $\partial T_{i1}/\partial x$ has been evaluated from a simple heat balance. The boundary conditions on equation (3) are

$$\frac{\partial T_{i1}}{\partial R} = -\frac{1}{2} \quad \text{at } R_i \quad (4a)$$

and

$$\frac{\partial T_{i1}}{\partial R} = 0 \quad \text{at } R_o \quad (4b)$$

The solution of equation (3) is a function of R only so that T_{i1} may be written

$$T_{i1} = \frac{4}{Re Pr} \frac{x^+}{b+1} + G(R) \quad (5)$$

In a similar way, for T_{o1} ,

$$\frac{1}{R} \frac{\partial}{\partial R} \left[\left(\frac{\epsilon_H}{v} + \frac{1}{Pr} \right) R \frac{\partial T_{o1}}{\partial R} \right] = \frac{2(b-1)}{(b+1)} \frac{r_o^+ u_o^+}{Re Pr} \quad (6)$$

with

$$\frac{\partial T_{o1}}{\partial R} = \frac{1}{2} \quad \text{at } R_o \quad (7a)$$

and

$$\frac{\partial T_{o1}}{\partial R} = 0 \quad \text{at } R_i \quad (7b)$$

The fully developed temperature for heating on the outer wall is thus

$$T_{o1} = \frac{4b}{b+1} \frac{x^+}{Re Pr} + H(R) \quad (8)$$

where $H(R)$ is the solution of equation (6).

For the developing case T_2 , a solution is found by separation of variables so that

$$T_2 = \sum_{n=1}^{\infty} C_n \phi_n \exp \left[-\frac{8\lambda_n^2}{Re} x^+ \right] \quad (9)$$

The equation for the eigenfunctions, ϕ_n is

$$\frac{\partial}{\partial R} \left[\left(\frac{\epsilon_H}{v} + \frac{1}{Pr} \right) R \frac{\partial \phi_n}{\partial R} \right] + \frac{b-1}{b} \frac{4r_o^+ u_o^+}{Re} \lambda_n^2 R \phi_n = 0 \quad (10)$$

with the boundary conditions that

$$\frac{\partial \phi_n}{\partial R} = 0 \quad \text{at } R_i \quad (11a)$$

and

$$\frac{\partial \phi_n}{\partial R} = 0 \quad \text{at } R_o \quad (11b)$$

The eigenconstants, C_n are determined from the Sturm-Liouville condition and since $T_2 = -T_1$ at $x = 0$, then

$$C_n = \frac{R_i}{R_o} \frac{\int_{R_o}^{R_i} -u_o^+ T_1 \phi_n R dR}{\int_{R_i}^{R_o} u_o^+ \phi_n^2 R dR} \quad (12)$$

Since the boundary conditions, equation (11), are the same at each surface the λ_n are identical whether heating is at R_i or R_o . Only one set of λ_n need to be determined from equation (10). The eigenfunctions and constants for heating at the inner wall, ϕ_n and C_n are however not the same as those for heating at the outer wall, ψ_n and D_n since equation (10) and T_o and T_i are not symmetric with respect to the centre line of the annular gap. Accordingly the further set of eigenconstants, D_n , need to be determined in order to evaluate T_{o2} . Thus T_{i2} is given by

$$T_{i2} = \sum_{n=1}^{\infty} C_n \phi_n \exp \left[-\frac{8\lambda_n^2}{Re} x^+ \right] \quad (13)$$

$$T_{o2} = \sum_{n=1}^{\infty} D_n \psi_n \exp \left[-\frac{8\lambda_n^2}{Re} x^+ \right] \quad (14)$$

where C_n are calculated from equation (12) with $T_1 = T_i$ and D_n from equation (12) with $T_1 = T_o$.

NUSSELT NUMBER

When the temperatures T_i and T_o are determined, the Nusselt numbers may be calcu-

lated as follows. For the inner wall,

$$Nu_i = \frac{hD}{k} = \frac{q_i}{t_i - t_b} \frac{D}{k} \tag{15}$$

If heating is only at R_i then equation (15) becomes

$$Nu_i = \frac{1}{\left[G(R) + \sum_{n=1}^{\infty} C_n \phi_n \exp\left(\frac{8\lambda_n^2}{Re} x^+\right) \right]} \tag{16}$$

Since the bulk temperature, defined as

$$t_b = \frac{\int_{R_i}^{R_o} u r dr}{\int_{R_i}^{R_o} u r dr} \tag{17}$$

Similarly for heating at R_o only

$$Nu_o = \frac{1}{H(R)_o \left[1 - \sum_{n=1}^{\infty} D_n \exp\left(-\frac{8\lambda_n^2}{Re} x^+\right) \right]} \tag{19}$$

If there are uniform heat fluxes at each side, which may be arbitrarily different, the Nusselt numbers may be calculated from the principle of superposition. Such cases for the parallel plate channel were given by Hatton and Quarmby [4]. Thus Nu_i with constant but arbitrary values of q_i and q_o at R_i and R_o respectively becomes

$$Nu_i = \frac{1}{G(R)_i \left[1 - \sum_{n=1}^{\infty} C_n \exp\left(-\frac{8\lambda_n^2}{Re} x^+\right) \right] - \frac{q_o}{q_i} \left[H(R)_i + \sum_{n=1}^{\infty} D_n (\psi_n)_i \exp\left(-\frac{8\lambda_n^2}{Re} x^+\right) \right]} \tag{20}$$

$$Nu_o = \frac{1}{H(R)_i \left[1 - \sum_{n=1}^{\infty} D_n \exp\left(-\frac{8\lambda_n^2}{Re} x^+\right) \right] - \frac{q_i}{q_o} \left[G(R)_o + \sum_{n=1}^{\infty} C_n (\phi_n)_o \exp\left(-\frac{8\lambda_n^2}{Re} x^+\right) \right]} \tag{21}$$

may also be regarded as the sum of two parts. So that for the fully developed part the difference between T_1 and T_{1b} is $G(R)_i$ whilst for the developing part it is easily seen from equation (10), that T_{2b} is zero. Further, in calculating C_n the starting value of ϕ_n at R_i is set equal to $-G(R)_i$ and equation (16) may thus be simplified to

$$Nu_i = \frac{1}{G(R)_i \left[1 - \sum_{n=1}^{\infty} C_n \exp\left(-\frac{8\lambda_n^2}{Re} x^+\right) \right]} \tag{18}$$

In equations (20) and (21) the sign convention on heat flux is that it is taken positive in the positive direction of R . It should be noted that the $(\phi_n)_o$ are not equal to $G(R)_o$ and need to be tabulated, as do the values of $(\psi_n)_i$, if Nu_i and Nu_o for arbitrary values of heat flux ratio are required.

DESCRIPTION OF THE VELOCITY PROFILE AND EDDY DIFFUSIVITY

The value of the solution to the present problem is much dependent on the accuracy of the equations which are used to describe the velocity profile and eddy diffusivity. The turbulent velocity profile in concentric annuli may be

formulated by an analysis given by [3]. In this analysis the flow is divided into an inner velocity profile, for $r_i < r < r_m$, and an outer profile, $r_o > r > r_m$. In each part the region of flow close to the wall, up to y_i^+ , is analysed from Deissler's [5] description of the eddy diffusivity. In the main stream, $y_i^+ < y^+ < y_m^+$, the eddy diffusivity is that given by [1], whilst the velocity profile is given by the analysis of [3].

Thus for the inner profile for $0 < y_i^+ < y_{ii}^+$

$$\frac{\varepsilon_m}{\nu} = n^2 u_i^+ y_i^+ [1 - \exp(-n^2 u_i^+ y_i^+)] \quad (22a)$$

and

$$\frac{du_i^+}{dy_i^+} = \frac{\tau/\tau_i}{1 + n^2 u_i^+ y_i^+ [1 - \exp(-n^2 u_i^+ y_i^+)]} \quad (22b)$$

with

$$u_i^+ = 0 \quad \text{at} \quad y_i^+ = 0.$$

For

$$y_{ii}^+ < y_i^+ < y_{mi}^+$$

$$\frac{d^2 u_i^+}{dy_i^{+2}} = \frac{-K(du_i^+/dy_i^+)^2}{[\tau/\tau_i - du_i^+/dy_i^+]^{\frac{1}{2}}} \quad (23)$$

and the ordinate and gradient of u_i^+ are matched between equations (22b) and (23). In the outer profile, for $0 < y_o^+ < y_{io}^+$

$$\frac{\varepsilon_m}{\nu} = n^2 u_o^+ y_o^+ [1 - \exp(-n^2 u_o^+ y_o^+)] \quad (24a)$$

and

$$\frac{du_o^+}{dy_o^+} = \frac{\tau/\tau_o}{1 + n^2 u_o^+ y_o^+ [1 - \exp(-n^2 u_o^+ y_o^+)]} \quad (24b)$$

whilst for $y_{io}^+ < y_o^+ < y_{mo}^+$

$$\frac{d^2 u_o^+}{dy_o^{+2}} = \frac{-K(du_o^+/dy_o^+)^2}{[\tau/\tau_o - du_o^+/dy_o^+]^{\frac{1}{2}}} \quad (25)$$

The boundary conditions on u_o^+ are similar to those on u_i^+ .

In integrating the equations of the velocity profile, values must be given to n^2 , y_i^+ and K .

It has been shown [3] that K may be taken as 0.36 whilst n^2 and y_i^+ are given by Fig. 1. As an example of the correctness of this analysis, Fig. 2 shows a comparison of its predictions with the experimental results of [2] for radius ratios 2.88 and 9.37.

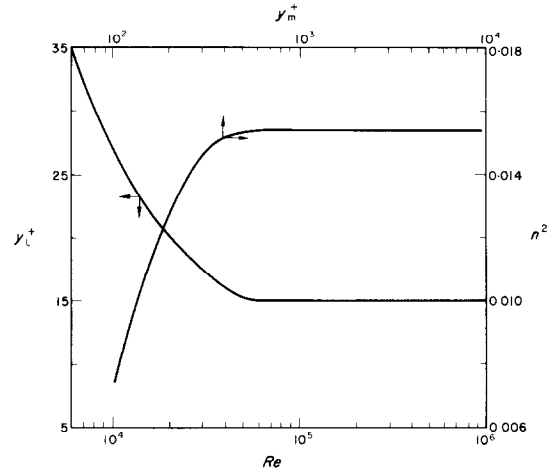


FIG. 1. Relationship between the parameters of the turbulent velocity profile.

It is possible to derive the eddy diffusivity for $y_i^+ < y^+ < y_m^+$, from the velocity profile given above. However, the resulting eddy diffusivity of momentum at y_m^+ is zero. The eddy diffusivity of heat, ε_H , is obtained from ε_m by a multiplicative factor, the ratio $\varepsilon_H/\varepsilon_m$. With the present boundary conditions, however, heat is being transferred across y_m^+ accordingly, a zero value for ε_H at y_m^+ is not acceptable.

Both [1] and [4] successfully used descriptions of the eddy diffusivity which did not strictly follow from the velocity profile but which avoided a zero value of ε_m at y_m^+ . Similarly, ε_m is described here by an equation for the inner profile

$$\begin{aligned} \frac{\varepsilon_m}{\nu} = & \frac{1}{15} \left(1 - \frac{a}{b}\right) r_o^+ (1 - \beta_i^2) (1 + 2\beta_i^2) \\ & \times \left[1 + 0.6 \sqrt{\left(\frac{\tau_o}{\tau_i}\right) \beta_i (1 - \beta_i)} \right] \\ & \times \left[1 - \left(1 - \frac{y_{mi}^+}{y_{mo}^+}\right) \beta_i \right] - C_i \quad (26) \end{aligned}$$

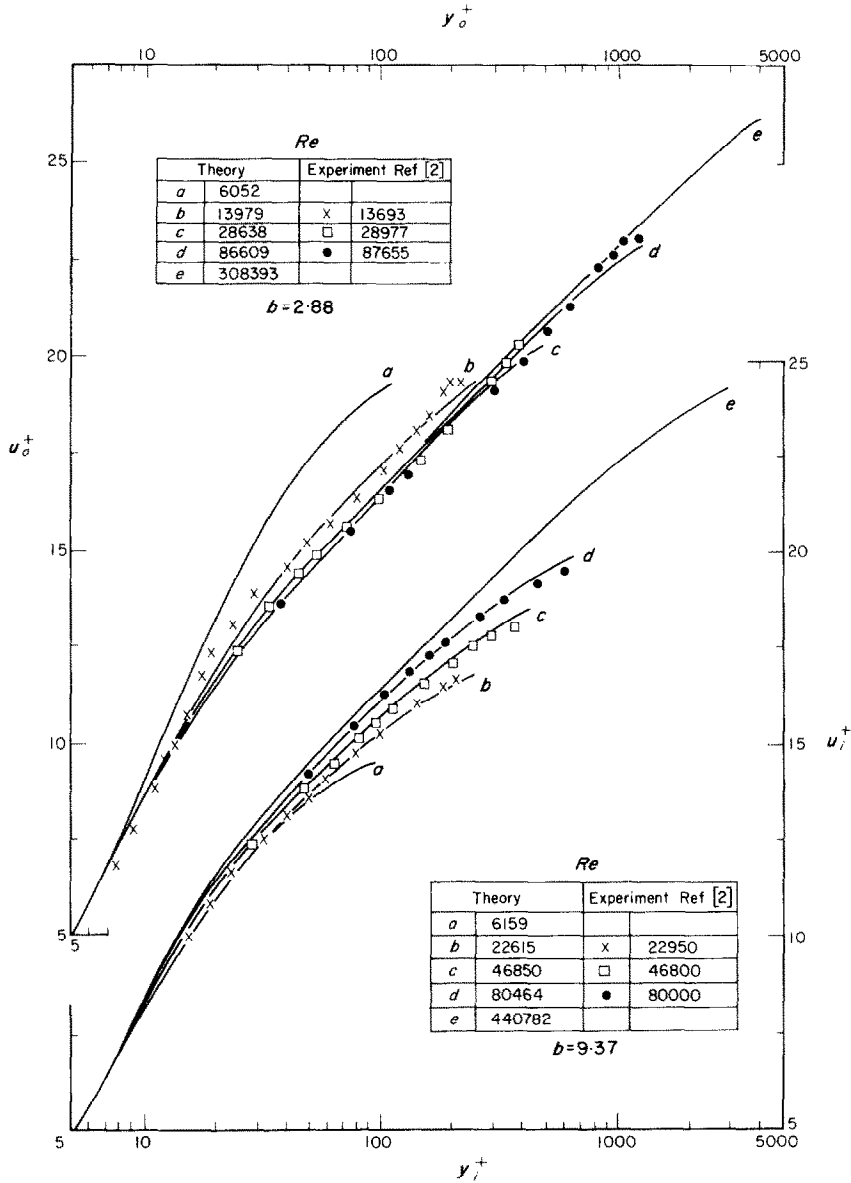


FIG. 2. Turbulent velocity profiles for radius ratios $b = 2.88$ and 9.37 .

and for the outer profile

$$\frac{\epsilon_m}{\nu} = \frac{1}{15} \left(1 - \frac{a}{b}\right) r_o^+ (1 - \beta_o^2) (1 + 2\beta_o^2) \times [1 + 0.6 \beta_o (1 - \beta_o^2)] - C_o. \quad (27)$$

Equations (26) and (27) with C_i and C_o both zero, were given by [1]. The constants have been introduced to eliminate the discontinuity which would otherwise occur in ϵ_m at y_i^+ . Thus if the difference at y_{ii}^+ between equations (22a) and

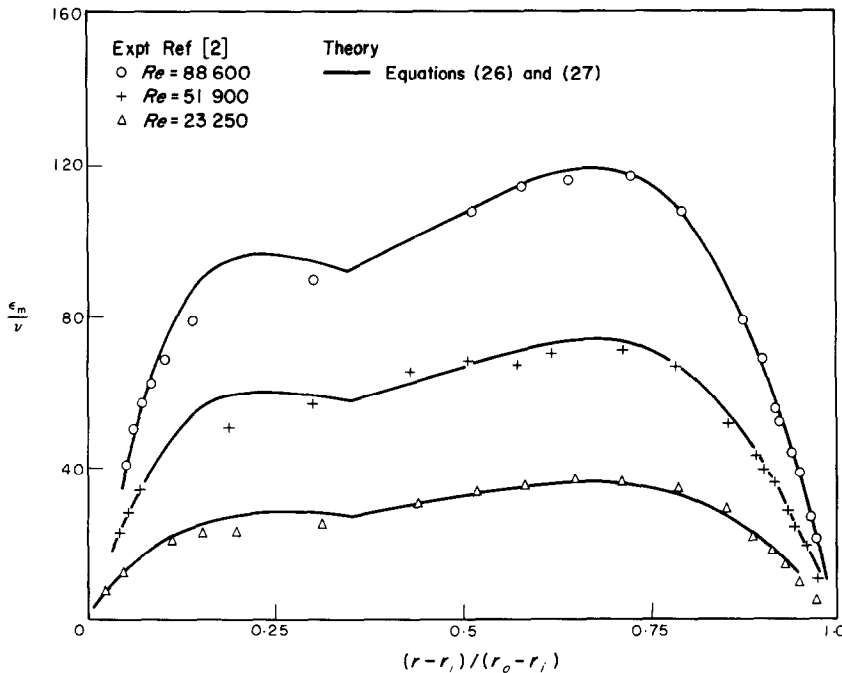


FIG. 3. Eddy diffusivity in concentric annuli $b = 5.62$.

(26) with $C_i = 0$ is $\delta(\epsilon_m)_i$ then

$$C_i = \frac{\delta(\epsilon_m)_i(y_{mi}^+ - y_i^+)}{(y_{mi}^+ - y_{ii}^+)}$$

and similarly

$$C_o = \frac{\delta(\epsilon_m)_o(y_{mo}^+ - y_i^+)}{(y_{mo}^+ - y_{io}^+)}$$

The agreement between these expressions and some of the experimental results of [2] is shown in Fig. 3. It has been shown [1] that this description of ϵ_m holds for b up to 19 and Reynolds numbers of 700000.

It is possible to generate the velocity profile from the eddy diffusivity expressions given above by use of the equation,

$$\frac{\tau}{\tau_w} = \left(1 + \frac{\epsilon_m}{\nu}\right) \frac{du^+}{dy^+} \tag{28}$$

However, the velocity profiles thus derived do not give good agreement with experiment.

Also, the velocity profile derived from the eddy diffusivity was considered by Leung *et al.* [1] to be too algebraically complex to use in treating the fully developed heat transfer situation. Calculations for this case by the present authors, [6], showed that the use of the present velocity profile and eddy diffusivity gives results for Reynolds numbers less than 30000 which are in better agreement with experiment than the results of Leung *et al.* These authors found their analysis disagreed with experiment about 10–15%. The results of reference [6] are in good agreement with experiment and this is due to the improvement in the description of the velocity profile since the eddy diffusivity is the same in both analyses. To use the velocity profile derived from the eddy diffusivity would clearly be even less satisfactory than the assumption of Leung *et al.* and would certainly lead to a disagreement with experiment of at least the same order as that mentioned. Therefore, the velocity profile and eddy diffusivity are

given by the expressions which provide the best agreement with experiment, although, they are not consistent according to equation (28). This approach is amply justified by the present results as well as those of [1], [4] and [6].

The eddy diffusivity of heat, ϵ_H , which is required in equation (6) is obtained from ϵ_m by the expression for their ratio due to Jenkins [8]. This may be expressed as:

$$\frac{\epsilon_H}{\epsilon_m} = Pr \left\{ \frac{1 - \frac{90}{\pi^6} \frac{lv'}{\alpha} \sum_{n=1}^{\infty} \frac{1}{n^6} \left[1 - \exp \left(- \frac{n^2 \pi^2 \alpha}{lv'} \right) \right]}{1 - \frac{90}{\pi^6} \frac{lv'}{v} \sum_{n=1}^{\infty} \frac{1}{n^6} \left[1 - \exp \left(- \frac{n^2 \pi^2 v}{lv'} \right) \right]} \right\} \quad (29)$$

and it has been evaluated by Leung *et al.* [1]. The relationship is shown in Fig. 4 for $Pr = 0.01, 0.7$ and 1000 .

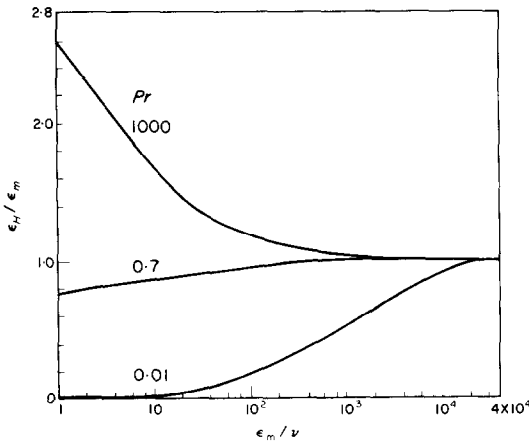


FIG. 4. Relationship between eddy diffusivity of heat and momentum.

CALCULATIONS AND RESULTS

In integrating the equations of the velocity profile and temperature, r_0^+ is chosen as the basic parameter for given values of the radius ratio. The choice of r_0^+ determines y_{mo}^+, y_{mi}^+ and

r_i^+ since it is easily shown from the expressions for shear stress in annuli, Knudsen and Katz [7], that

$$y_{mo}^+ = \left(1 - \frac{a}{b} \right) r_0^+ \quad (30)$$

$$y_{mi}^+ = \frac{a - 1}{b} \frac{b(a^2 - 1)}{(b^2 - a^2)} r_0^+ \quad (31)$$

$$r_i^+ = \frac{1}{b} \frac{b(a^2 - 1)}{(b^2 - a^2)} r_0^+. \quad (32)$$

Also, the Reynolds number is determined by the choice of r_0^+ since $Re = u_b D / \nu$ becomes

$$Re = \frac{4}{b + 1} \left[\frac{1}{r_i^+} \int_0^{y_{mi}^+} u_i^+ (y_i^+ + r_i^+) dy_i^+ + \frac{b}{r_o^+} \int_0^{y_{mo}^+} u_o^+ (r_o^+ - y_o^+) dy_o^+ \right]. \quad (33)$$

The relationship between r_o^+ and Re for the radius ratios $b = 2.88, 5.67, 9.37$ and 50 is given in Table 1 and shown in Fig. 5. The ratios were taken to agree with the results of [2] or, for $b = 50$, since a comparison may be made with results for a circular tube. The eigenvalues and constants C_n and D_n for $b = 2.88, 5.67$ and 9.37 are given in Table 2 for $Pr = 0.01$ and 1000 for various Reynolds numbers. Table 3 gives those for $Pr = 0.7$ together with $(\phi_n)_o$ and $(\psi_n)_i$. The results required for calculating the fully developed heat transfer situation namely $G(R)_i$,

Table 1. Relationship between r_0^+ and Reynolds number

$b = 1.05$		2.88		5.625		9.37		50	
r_0^+	Re	r_0^+	Re	r_0^+	Re	r_0^+	Re	r_0^+	Re
6000	9050	915	20363	1020	30226	325	9243	295	9088
11100	17530	2800	73035	2000	65116	1280	42945	1000	36310
29600	52900	4400	122275	3550	125267	2200	80016	2210	89640
50000	96650	5900	170415	6250	236622	4000	157789	2500	103140
100000	212200	7500	223200	7300	290900	5650	231996	5000	225600
150000	334600	10000	308400	10000	401200	10000	440800	10000	488900

Table 2. Eigenvalues and constants for $Pr = 0.01$ and 1000

b	Re	n	$Pr = 0.01$			$Pr = 1000$		
			λ_n	C_n	D_n	λ_n	C_n	D_n
2.880	20363	1	24.17731	0.506509	0.536527	14.45994	0.002380	0.002498
		2	46.54429	0.159386	0.153502	27.59629	0.001751	0.002248
		3	68.99162	0.076777	0.073212	39.17500	0.003944	0.005021
		4	91.51116	0.045710	0.042671	49.54510	0.015811	0.027773
		5	113.98930	0.030338	0.028196	64.78665	0.111750	0.069435
		6	136.52980	0.021646	0.020065	73.02547	0.044796	0.043102
	73035	1	25.29953	0.511772	0.531962	23.98821	0.002179	0.002225
		2	48.72858	0.158844	0.159019	45.86473	0.000905	0.001081
		3	71.92987	0.079757	0.076528	65.85810	0.000803	0.000848
		4	95.22695	0.047167	0.044779	85.48402	0.000804	0.000891
		5	118.60790	0.031418	0.029365	105.18070	0.000988	0.001105
		6	142.02810	0.022026	0.020731	124.52670	0.001426	0.001680
5.625	122275	1	27.01410	0.504429	0.517427	29.38546	0.002230	0.002264
		2	51.99779	0.157097	0.161956	56.13826	0.000870	0.001028
		3	76.43619	0.082024	0.079370	80.59538	0.000698	0.000720
		4	100.95710	0.049280	0.047148	104.63000	0.000603	0.000642
		5	125.65310	0.032750	0.031006	128.83100	0.000602	0.000632
		6	150.35460	0.023304	0.021926	152.71130	0.000657	0.000702
	170415	1	28.77439	0.496065	0.503574	33.50904	0.002279	0.002308
		2	55.34156	0.155295	0.163953	63.98510	0.000868	0.001022
		3	81.05700	0.084043	0.081713	91.84416	0.000670	0.000687
		4	106.84350	0.050982	0.049212	119.22030	0.000548	0.000577
		5	132.89120	0.034070	0.032463	146.80670	0.000506	0.000524
		6	158.91790	0.024328	0.023016	174.04800	0.000502	0.000523
5.625	30226	1	25.08594	0.449889	0.523782	18.23451	0.001592	0.002065
		2	47.32277	0.165040	0.157258	33.60291	0.001022	0.001554
		3	69.57955	0.085758	0.075879	48.01757	0.001514	0.002185
		4	91.99697	0.052219	0.044724	61.67214	0.003365	0.005523
		5	114.44040	0.035440	0.029486	74.49123	0.011909	0.032425
		6	136.89560	0.025528	0.021023	93.42820	0.142819	0.045725
	65116	1	26.16003	0.449775	0.514758	24.78381	0.001530	0.001954
		2	49.15878	0.164516	0.162450	45.57530	0.000768	0.001099
		3	72.09828	0.087774	0.078854	65.26735	0.000742	0.000927
		4	95.16327	0.054018	0.046346	84.31973	0.000854	0.001035
		5	118.33040	0.036406	0.030519	103.39960	0.000112	0.001478
		6	141.55760	0.026113	0.021602	122.31280	0.001854	0.002669

Table 2. (continued)

<i>b</i>	<i>Re</i>	<i>n</i>	<i>Pr</i> = 0.01			<i>Pr</i> = 1000		
			λ_n	C_n	D_n	λ_n	C_n	D_n
5.625	125267	1	28.65356	0.438576	0.493071	32.12308	0.001559	0.001979
		2	53.54745	0.161767	0.167460	58.96135	0.000723	0.001011
		3	78.21252	0.090353	0.083010	84.41085	0.000609	0.000723
		4	102.91460	0.057096	0.049314	109.07830	0.000574	0.000635
		5	127.79640	0.038567	0.032754	133.88340	0.000568	0.000647
		6	152.78930	0.027755	0.023179	158.67630	0.000631	0.000723
	236622	1	33.43689	0.416635	0.459313	41.61860	0.001619	0.002030
		2	61.99852	0.157116	0.172983	76.18190	0.000723	0.001013
		3	89.98067	0.093993	0.088790	108.92890	0.000576	0.000672
		4	117.84760	0.061790	0.053850	140.71410	0.000499	0.000532
		5	146.04040	0.041965	0.036267	172.75980	0.000436	0.000474
		6	174.43460	0.030422	0.025774	204.82190	0.000416	0.000445
9.370	42945	1	26.08409	0.396769	0.512191	22.23787	0.001077	0.001865
		2	48.45535	0.162971	0.161145	39.98038	0.000685	0.001257
		3	70.81297	0.091726	0.078031	57.03172	0.000817	0.001352
		4	93.29051	0.058328	0.046089	73.46363	0.001311	0.002128
		5	115.87760	0.040366	0.030512	89.53074	0.002661	0.005318
		6	138.48150	0.029687	0.021729	104.94100	0.007770	0.027661
	80016	1	27.69430	0.392030	0.500096	28.47057	0.001059	0.001825
		2	51.12011	0.163344	0.166700	51.06734	0.000596	0.001048
		3	74.49731	0.094370	0.081673	72.84718	0.000568	0.000849
		4	97.95088	0.061297	0.048454	93.96866	0.000652	0.000868
		5	121.51710	0.042552	0.031992	114.89270	0.000802	0.001094
		6	145.16780	0.031105	0.022752	135.85500	0.001121	0.001679
157789	1	31.42485	0.372042	0.470353	37.33033	0.001081	0.001864	
	2	57.42105	0.158791	0.172075	66.82310	0.000573	0.000986	
	3	83.27494	0.086417	0.086798	95.26581	0.000491	0.000697	
	4	109.12415	0.065134	0.051904	122.87460	0.000482	0.000585	
	5	135.09450	0.045795	0.034663	150.27890	0.000477	0.000563	
	6	161.24110	0.033460	0.024721	177.85890	0.000496	0.000594	
231996	1	34.99826	0.354984	0.446835	43.91007	0.001099	0.001885	
	2	63.48927	0.155014	0.175169	78.35333	0.000573	0.000992	
	3	91.71190	0.098016	0.090506	111.58120	0.000479	0.000672	
	4	119.84640	0.068318	0.054671	143.88570	0.000450	0.000531	
	5	148.11630	0.048515	0.036834	175.99190	0.000418	0.000477	
	6	176.65020	0.035465	0.026397	208.32320	0.000400	0.000461	

Table 3. Eigenvalues and constants and some relevant values of the eigenfunctions for *Pr* = 0.7

<i>b</i>	<i>Re</i>	$(\phi_n)_i$	$(\psi_n)_o$	<i>n</i>	λ_n	C_n	D_n	$(\psi_n)_i$	$(\phi_n)_o$
20363	-0.018893	-0.021002	1	12.29422	0.244374	0.243016	0.033900	0.011705	
			2	23.61494	0.087828	0.102117	-0.031351	-0.012657	
			3	33.88883	0.064358	0.065161	0.033597	0.011811	
			4	43.98521	0.049049	0.051260	-0.033068	-0.012000	
			5	54.08981	0.041928	0.042427	0.033606	0.011808	
			6	63.98431	0.037162	0.037994	-0.033433	-0.011869	
2.880	-0.007056	-0.007665	1	21.42147	0.220882	0.218559	0.012548	0.004310	
			2	40.92032	0.080462	0.093960	-0.011548	-0.004683	
			3	58.54501	0.059056	0.059218	0.012465	0.004339	
			4	75.84360	0.043684	0.044898	-0.012309	-0.004304	
			5	93.27797	0.035202	0.035029	0.012513	0.004322	
			6	110.49490	0.029042	0.028930	-0.012503	-0.004326	

Table 3. (continued)

b	Re	$(\phi_n)_i$	$(\psi_n)_o$	n	λ_n	C_n	D_n	$(\psi_n)_i$	$(\phi_n)_o$
122275	-0.004772	-0.005152		1	26.75531	0.211098	0.208295	0.008472	0.002902
				2	51.04889	0.077396	0.090670	-0.007774	-0.003163
				3	72.96553	0.057293	0.057364	0.008410	0.002923
				4	94.47098	0.042484	0.043605	-0.008305	-0.002960
				5	116.16890	0.034245	0.034049	0.008440	0.002913
				6	137.58940	0.028304	0.028147	-0.008438	-0.002914
170415	-0.003694	-0.003975		1	30.93261	0.205009	0.201967	0.006552	0.002241
				2	58.97714	0.075512	0.088632	-0.006002	-0.002446
				3	82.24569	0.049809	0.049919	0.010037	0.003420
				4	109.02850	0.041797	0.042874	-0.006421	-0.002207
				5	134.04560	0.033704	0.033496	0.006524	0.002251
				6	158.74340	0.027871	0.027690	-0.006524	-0.002251
30226	-0.011643	-0.014557		1	15.80482	0.189589	0.215398	0.028969	0.005851
				2	29.10876	0.079778	0.103105	-0.027159	-0.006241
				3	41.62592	0.060754	0.065299	0.029784	0.005691
				4	53.75438	0.049190	0.048635	-0.031051	-0.005458
				5	65.99565	0.039876	0.039598	0.030987	0.005470
				6	78.20838	0.034712	0.033384	-0.031484	-0.005383
65116	-0.006637	-0.008078		1	22.12897	0.172553	0.199054	0.016173	0.003315
				2	40.59051	0.074302	0.096606	-0.015228	-0.003521
				3	57.94711	0.057121	0.061577	0.016730	0.003205
				4	74.71628	0.046418	0.045595	-0.017519	-0.003061
				5	91.61295	0.037143	0.036586	0.017503	0.003063
				6	108.51530	0.031451	0.029879	-0.017814	-0.003010
5.625	125267	-0.004081	-0.004889	1	29.41051	0.161243	0.186616	0.009849	0.002025
				2	53.80256	0.070380	0.092116	-0.009257	-0.002155
				3	76.71229	0.054759	0.059023	0.010206	0.001955
				4	98.83295	0.044791	0.043761	-0.010714	-0.001862
				5	121.13560	0.035833	0.035216	0.010689	0.001866
				6	143.45770	0.030346	0.028808	-0.010869	-0.001835
236622	-0.002509	-0.002966		1	39.00530	0.150936	0.175272	0.006006	0.001239
				2	71.19002	0.066805	0.087950	-0.005639	-0.001320
				3	101.38650	0.052606	0.056720	0.006233	0.001194
				4	130.50820	0.043398	0.042233	-0.006558	-0.001135
				5	159.87200	0.034752	0.034063	0.006537	0.001139
				6	189.29200	0.029422	0.027908	-0.006643	-0.001121
42945	-0.007761	-0.010809		1	19.63342	0.137751	0.197021	0.023447	0.003578
				2	35.18177	0.067790	0.100076	-0.023073	-0.003636
				3	50.07657	0.053737	0.064539	0.025587	0.003279
				4	64.48936	0.046975	0.047032	-0.028016	-0.002995
				5	78.93936	0.039701	0.037841	0.027389	0.002808
				6	93.32502	0.033478	0.031208	-0.029034	-0.002890
80016	-0.004981	-0.006753		1	25.69178	0.127153	0.184795	0.014722	0.002285
				2	45.89372	0.063675	0.095471	-0.014502	-0.002319
				3	65.25497	0.051096	0.061719	0.016148	0.002083
				4	83.97887	0.045174	0.045253	-0.017743	-0.001896
				5	102.57160	0.038173	0.036230	0.018216	0.001846
				6	121.31750	0.032365	0.030112	-0.018411	-0.001827
9.370	157789	-0.003021	-0.004001	1	34.63892	0.117118	0.172911	0.008759	0.001380
				2	61.68753	0.059761	0.090705	-0.008637	-0.001390
				3	87.58350	0.048730	0.059107	0.009664	0.001251
				4	112.60460	0.043532	0.043328	-0.010665	-0.001133
				5	137.44720	0.036893	0.034827	0.010955	0.001103
				6	162.51850	0.031186	0.028943	-0.011044	-0.001094

Table 3. (continued)

b	Re	$(\phi_n)_i$	$(\psi_n)_o$	n	λ_n	C_n	D_n	$(\psi_n)_i$	$(\phi_n)_o$
231996	-0.002256	-0.002951		1	41.20603	0.111670	0.166341	0.006472	0.001029
				2	73.26697	0.057625	0.088018	-0.006390	-0.001042
				3	103.94400	0.047413	0.057629	0.007165	0.000929
				4	133.56570	0.042649	0.042348	-0.007925	-0.000840
				5	162.96340	0.036254	0.034114	0.008144	0.000817
				6	192.64480	0.030621	0.028394	-0.008200	-0.000812

Table 4. Values of the inner and outer fully developed temperature solutions at the annulus walls

b	Pr	0.01		0.7		1000	
		$G(R)_i$	$G(R)_o$	$G(R)_i$	$G(R)_o$	$G(R)_i$	$G(R)_o$
2.880	20363	0.143354	-0.037779	0.018893	-0.002184	0.001252	-0.000001
	73035	0.133455	-0.034407	0.007056	-0.000723	0.000416	-0.000000
	122275	0.121309	-0.030332	0.004772	-0.000465	0.000266	-0.000000
	170415	0.110607	-0.026883	0.003694	-0.000348	0.000199	-0.000000
5.625	30226	0.111770	-0.021005	0.011643	-0.000835	0.000848	-0.000002
	65116	0.106367	-0.019230	0.006638	-0.000414	0.000440	-0.000002
	125267	0.094683	-0.016080	0.004081	-0.000235	0.000250	-0.000000
	236622	0.077065	-0.012037	0.002509	-0.000134	0.000143	-0.000000
9.370	42945	0.086550	-0.012551	0.007761	-0.000345	0.000598	-0.000000
	80016	0.080512	-0.011595	0.004981	-0.000202	0.000354	-0.000000
	157789	0.069540	-0.008110	0.003021	-0.000112	0.000197	-0.000000
	231996	0.060929	-0.007120	0.002256	-0.000079	0.000141	-0.000000
50.000	36311	0.030715	-0.002428	0.004830	-0.000065	0.000546	-0.000000
	89645	0.027842	-0.001982	0.002690	-0.000030	0.000267	-0.000000
	103142	0.027126	-0.001884	0.002453	-0.000026	0.000238	-0.000000
	222160	0.021970	-0.001262	0.001438	-0.000013	0.000124	-0.000000
2.880		$H(R)_i$	$H(R)_o$	$H(R)_i$	$H(R)_o$	$H(R)_i$	$H(R)_o$
	20363	-0.108831	0.168257	-0.006289	0.021002	-0.000004	0.001359
	73035	-0.099541	0.151876	-0.002086	0.007665	-0.000002	0.000444
	122275	-0.087669	0.136049	-0.001339	0.005153	-0.000001	0.000283
5.625	170415	-0.077590	0.122818	-0.001002	0.003975	-0.000001	0.000211
	30226	-0.118407	0.158087	-0.005338	0.014557	-0.000060	0.000968
	65116	-0.109436	0.146226	-0.002338	0.008078	-0.000002	0.000493
	125267	-0.091997	0.126711	-0.001330	0.004889	-0.000001	0.000278
9.370	236622	-0.068644	0.100182	-0.000758	0.002966	-0.000001	0.000158
	42945	-0.118844	0.149015	-0.003243	0.010809	-0.000003	0.000709
	80016	-0.106312	0.135045	-0.001882	0.006753	-0.000002	0.000413
	157789	-0.083754	0.112449	-0.001052	0.004001	-0.000001	0.000227
50.000	231996	-0.068252	0.096473	-0.000746	0.002951	-0.000001	0.000161
	36311	-0.121528	0.143146	-0.003342	0.011954	-0.000003	0.000830
	89645	-0.099153	0.122806	-0.001504	0.005961	-0.000002	0.000374
	103142	-0.094252	0.118430	-0.001332	0.005355	-0.000002	0.000331
222160	-0.063065	0.089684	-0.000661	0.002921	-0.000001	0.000165	

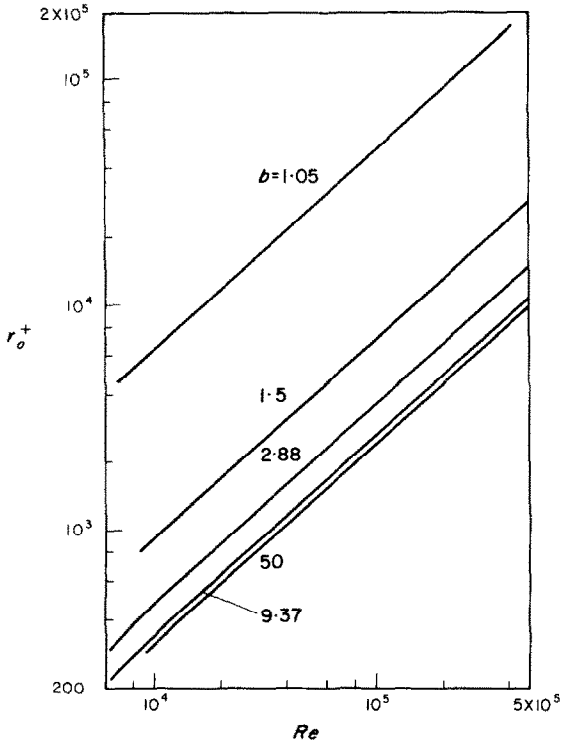


FIG. 5. Relationship between r_0^+ and the Reynolds number.

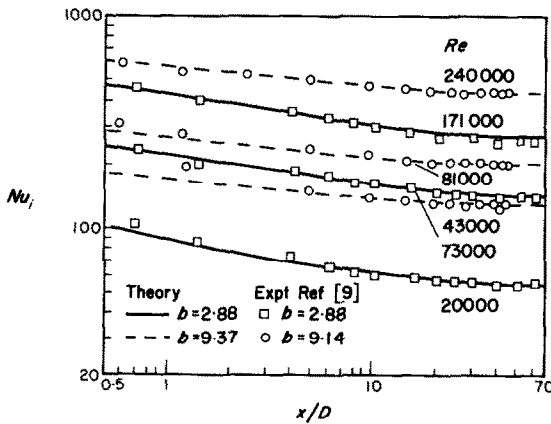


FIG. 6. Comparison between theory and experiment for entrance region heat transfer.

$G(R)_o$, $H(R)_i$ and $H(R)_o$ are given in Table 4 together with some results for $b = 50$.

COMPARISON WITH EXPERIMENT

The calculated values of the Nusselt number for heating of the core tube for $b = 2.88$ and 9.37 , are compared in Fig. 6 with the experimental results for $b = 2.88$ and $b = 9.17$ given

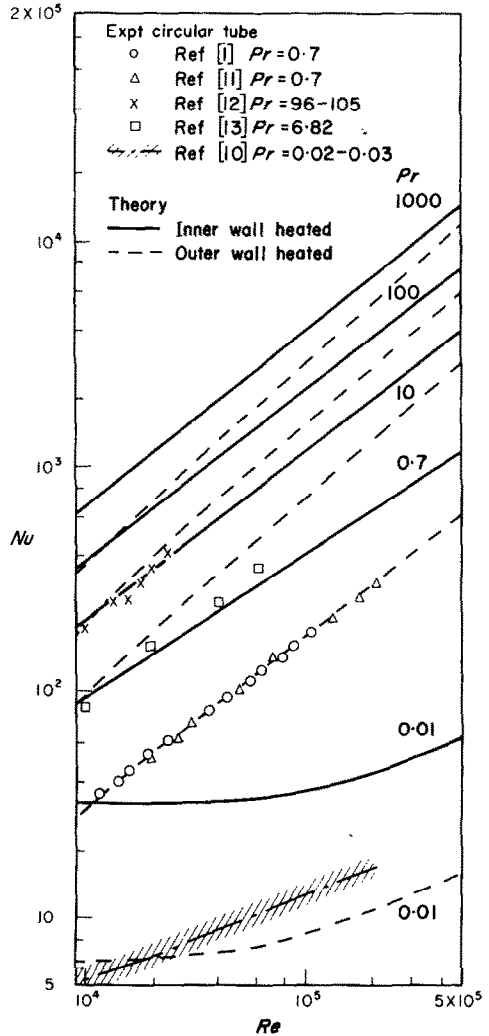


FIG. 7. Fully developed heat transfer for radius ratio $b = 50$.

by Quarmby [9] for air. The agreement is quite satisfactory. Experimental results for annuli for other Prandtl numbers are very sparse and

are not strictly comparable because of the differing boundary conditions. However, it is possible to make a comparison between the results of the present analysis for radius ratio $b = 50$ with heating on the outer wall only and certain experimental results for fully developed heat transfer in a circular tube with a uniform heat flux boundary condition.

This is shown in Fig. 7 where a comparison is made with results for liquid metals, $Pr = 0.02-0.03$; air, $Pr = 0.7$; water, $Pr = 6.82$; and ethyl glycol, $Pr = 96-105$. The agreement is satisfactory, especially for $Pr = 0.7$.

Reynolds number on the results as the experiments do. The correct Reynolds number and radius ratio effect is predicted, however. The effect of radius ratio on the entrance length for heating at the inner wall is shown in Fig. 9 together with results for heating at the outer wall. The results were obtained by cross-plotting from the calculated values for the chosen values of Reynolds number, $Re = 50000, 100000$ and 150000 . It may be seen that the radius ratio effect is much greater on the inner wall but the entrance length appears to become independent of Reynolds number for higher values.

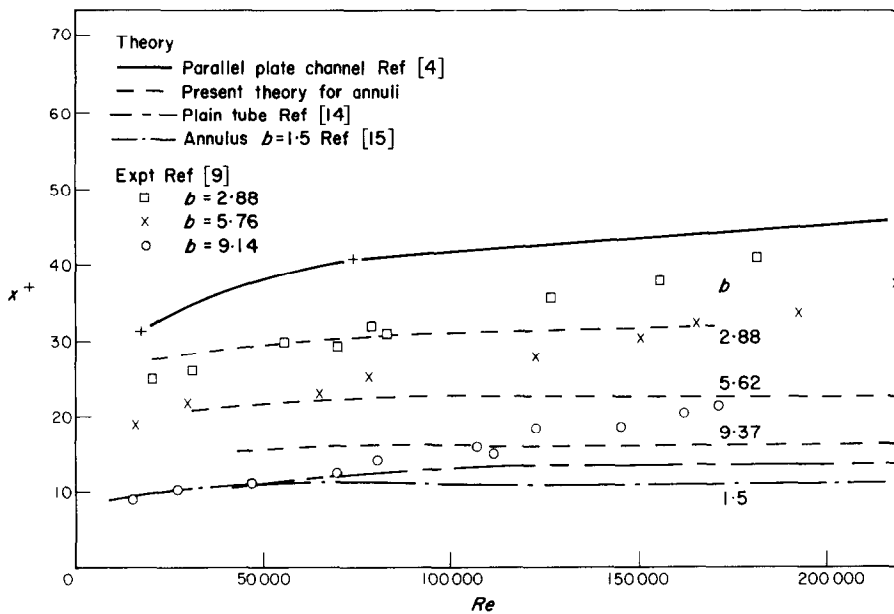


FIG. 8. Comparison between theory and experiment for the length of the entrance region.

It is important to know the length of the entrance region. This may be defined as the distance along the duct at which the Nusselt number has a value 5 per cent greater than its fully developed value. A comparison is given in Fig. 8 of the present analysis and some measurements of [9] for heating on the inner wall. There is reasonable agreement but the theoretical prediction does not show as much effect of

There is a considerable Prandtl number effect on the entrance length. This is shown in Fig. 10 where results for $b = 5.62$ are compared with the calculations of [4] for the parallel plate passage and Sparrow *et al.* [14] for the round tube. To make the comparison valid, results for heating the outer wall are shown. There is good agreement between the calculations for the three configurations. It may be seen that the

effects of radius ratio and Reynolds number become insignificant for Prandtl numbers greater than about 10 and the entrance lengths are very short for high Prandtl numbers.

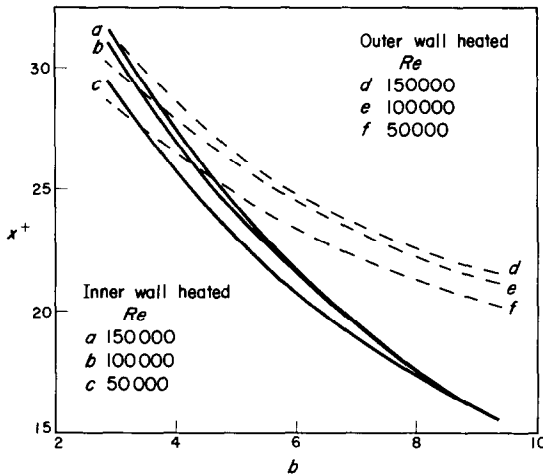


FIG. 9. Effect of radius ratio on the entrance length.

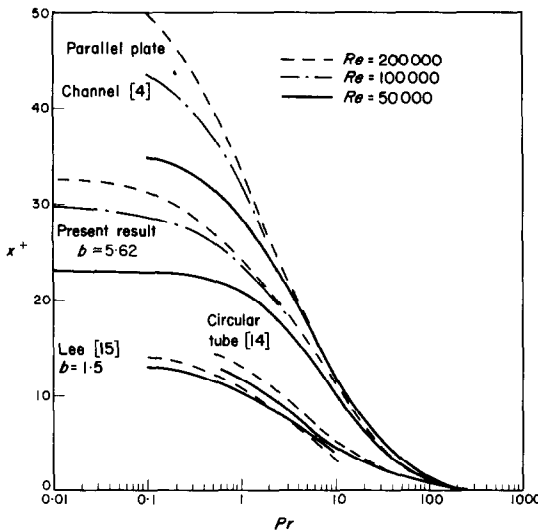


FIG. 10. Effect of Prandtl number on the entrance length.

Recently, Lee [15] has given a solution for heat transfer from the inner wall with a uniform heat flux. The solution was obtained using a boundary layer model and integral methods.

This method is not as satisfactory as the present method since arbitrary axial variations of wall heat flux cannot be handled by the principle of superposition but require each to have a separate solution. The description of the annular velocity profile which Lee [15] used is not in agreement with the experiments of either Quarmby [2] or Brighton and Jones [16]. For example, Lee assumed that the radius of maximum velocity is the same in turbulent flow as in laminar flow and no account was taken of the Reynolds number and radius ratio dependence of the $u^+ \sim y^+$ profile. It was assumed that the ratio of ε_H to ε_m is unity for Prandtl numbers of 10 and 0.1.

Lee's results for the fully developed Nusselt number are not in agreement with the measurements of [1] or [9]. The prediction of the entrance length for a radius ratio of 1.5 differs by about a factor of four from the measurements of [3] for $b = 2.88$ and from the theoretical prediction of the entrance length in a parallel plate channel, $b = 1$, given by [4]. Since a radius ratio of 1.5 is not greatly different to a parallel plate channel this discrepancy is significant. Lee's results may also be shown on Fig. 10. The effect of Prandtl number is correctly predicted but there is poor agreement with the present calculations and those of [4] and [14]. Also Lee's results predict a reversal of the Reynolds number effect at $Pr = 10$ which is not shown in the other results. Without lengthy calculation it is not possible to say exactly how the discrepancies in Lee's results arise, whether from the inaccuracy of the description of velocity and eddy diffusivity or from the integral method of calculation which was used.

CONCLUSIONS

There is good agreement between the analysis and experimental results for the entrance region for the range of radius ratios and Reynolds numbers considered, for $Pr = 0.7$. For other values of Prandtl number, the lack of suitable experimental data precludes a proper test of the entrance region solution. However, results for

the fully developed case for a radius ratio of fifty are in reasonable agreement with experiments for a plain tube. This indicates that the analysis and its assumptions are valid for high values of radius ratio and suggests that they are also valid for Prandtl numbers other than 0.7.

Calculations of the thermal entrance length, defined as the distance required for the Nusselt number to reach a value 1.05 times its ultimate value, are in good agreement with calculated results for the parallel plate channel and plain tube given in the literature. The entrance length is considerably decreased for Prandtl numbers greater than unity. The effect of increasing the radius ratio is to decrease the entrance length. The effect of increasing the Reynolds number is to increase the entrance length. The Reynolds number effect is not very great for the higher radius ratios.

From the agreement between theory and experiment it is considered that the solutions obtained for uniform heat flux are accurate and that they may be used to give the solution to practical problems in which there are arbitrary axial variation of the boundary conditions.

REFERENCES

1. E. Y. LEUNG, W. M. KAYS and W. C. REYNOLDS, Heat transfer and turbulent flow in concentric and eccentric annuli with constant and variable heat flux, Engng Report AHT4, Stanford University (1962).
2. A. QUARMBY, An experimental study of turbulent flow through concentric annuli, *Int. J. Mech. Sci.* **9**, 205 (1967).
3. A. QUARMBY, An analysis of turbulent flow in concentric annuli, *Appl. Scient. Res.* **19**, 250 (1968).
4. A. P. HATTON and A. QUARMBY, The effect of axially varying and unsymmetric boundary conditions on heat transfer between parallel plates, *Int. J. Heat Mass Transfer* **6**, 903 (1963).
5. R. C. DEISSLER, Analysis of turbulent heat transfer, mass transfer and fluid friction in smooth tubes at high Prandtl and Schmidt numbers, N.A.C.A. Report 1210 (1955).
6. A. QUARMBY and R. K. ANAND, Fully developed turbulent heat transfer in concentric annuli with uniform wall heat fluxes. To be published in *Chem. Engng Sci.*
7. J. G. KNUDSEN and D. L. KATZ, *Fluid Dynamics and Heat Transfer*. McGraw Hill, New York (1958).
8. R. JENKINS, Variation of the eddy conductivity with Prandtl modulus and its use in prediction of turbulent heat transfer coefficients, Heat Transfer and Fluid Mechanics Institute, p. 147. Stanford University Press, Stanford, California (1951).
9. A. QUARMBY, Some measurements of turbulent heat transfer in the thermal entrance region of concentric annuli, *Int. J. Heat Mass Transfer* **10**, 267 (1967).
10. B. LUBARSKY and S. J. KAUFMAN, Review of experimental investigations of liquid metal heat transfer, N.A.C.A. TN 3366 (1955).
11. R. G. DEISSLER, An analytical investigation of turbulent flow in smooth tubes with heat transfer with variable fluid properties, N.A.C.A. TN 2242 (1950).
12. H. KATO, H. NISHIJUAKI and N. HIROTA, Turbulent heat transfer in smooth tubes at high Prandtl numbers, *Proc. Eleventh Int. Congr. Appl. Mech.* p. 1101 (1964).
13. R. A. SEBAN and D. F. CASEY, Heat transfer to lead bismuth in turbulent flow in an annulus, *Trans. Am. Soc. Mech. Engrs* **79**, 1514 (1957).
14. E. M. SPARROW, T. M. HALLMAN and R. SEIGEL, Turbulent heat transfer in the thermal entrance region of a pipe with uniform heat flux, *Appl. Scient. Res.* **7**, 37 (1958).
15. Y. LEE, Turbulent heat transfer from the core tube in thermal entrance regions of concentric annuli, *Int. J. Heat Mass Transfer* **11**, 509 (1968).
16. J. A. BRIGHTON and J. B. JONES, Fully developed turbulent flow in annuli, *J. Bas. Engng* **86**, 835 (1964).

TRANSPORT DE CHALEUR TURBULENT DANS LA REGION D'ENTREE THERMIQUE DE TUYAUX ANNULAIRES CONCENTRIQUES AVEC FLUX DE CHALEUR PARIETAL UNIFORME

Résumé—Le problème du transport de chaleur turbulent dans des conduites annulaires concentriques est analysé dans le cas où il y a un flux de chaleur uniforme sur chaque surface annulaire. On donne la solution pour la région d'entrée thermique et le régime entièrement établi qui peut être étendue, grâce au principe de superposition, aux cas où il y a des variations axiales du flux de chaleur pariétal sur les deux surfaces annulaires.

Les solutions sont données pour les rapports des rayons égaux à 2,88; 5,625; 9,37 et 50 avec des nombres de Reynolds de 20000 à 240000 et pour $Pr = 0,01$; 0,7 et 1000. Il y a un bon accord avec les résultats expérimentaux pour des conduites annulaires pour $Pr = 0,7$ tandis que certains résultats, pour un rapport des rayons égal à 50, sont comparables favorablement avec les résultats pour un tube circulaire avec d'autres nombres de Prandtl.

TURBULENTER WÄRMEÜBERGANG IM GEBIET DES THERMISCHEN EINLAUFS VON KONZENTRISCHEN RINGSPALTEN MIT KONSTANTER WÄRMESTROMDICHTHE.

Zusammenfassung—Das Problem des turbulenten Wärmeübergangs in konzentrischen Ringspalten wird untersucht für den Fall konstanter Wärmestromdichte an eine der Ringoberflächen. Lösungen werden angegeben für das Gebiet des thermischen Einlaufs und für die ausgebildete Strömung. Sie können durch Superposition ausgedehnt werden, auf Fälle mit willkürlicher Wärmestromverteilung an beiden Ringflächen.

Die Lösungen gelten für die Radienverhältnisse 2,88; 5,625; 9,37 und 50 bei Reynoldszahlen von 20000 bis 240000 und Prandtlzahlen von 0,01; 0,7 und 1000. Für $Pr = 0,7$ ist die Übereinstimmung mit experimentellen Ergebnissen gut, für ein Radienverhältnis von 50 lassen sich einige Ergebnisse auch für andere Prandtlzahlen sehr gut mit Werten für das Rohr mit Kreisquerschnitt vergleichen.

ТЕПЛООБМЕН ПРИ ТУРБУЛЕНТНОМ ТЕЧЕНИИ ВО ВХОДНОЙ ТЕРМИЧЕСКОЙ ОБЛАСТИ КОНЦЕНТРИЧЕСКИХ КАНАЛОВ ПРИ РАВНОМЕРНОМ ТЕПЛОВОМ ПОТОКЕ НА СТЕНКЕ

Аннотация—Анализируется задача теплообмена при турбулентном течении в концентрических каналах при равномерном тепловом потоке на каждой кольцевой поверхности. Получено решение для входной термической области и полностью развитого течения, которое методом суперпозиции можно применить к случаям произвольных изменений теплового потока на стенке вдоль оси на обоих кольцевых поверхностях.

Решения получены для отношений радиусов 2,88; 5,625; 9,37 и 50 при числах Рейнольдса от 20 000 до 240 000 и при $Pr = 0,01; 0,7$ и 1000. Имеется хорошее соответствие с экспериментальными результатами для каналов при $Pr = 0,7$. Результаты для отношения радиусов, равном 50, сравниваются с результатами для круглой трубы при других числах Прандтля.